Temperature analysis of low-expansion Fabry-Perot cavities

Richard W. Fox

National Institute of Standards and Technology,325 Broadway, Boulder, CO 80305, USA
richard.fox@nist.gov

Abstract: Temperature dependent structural distortion at the contacted mirrors of low-expansion glass cavities can introduce changes to the cavity length independent of the length of the spacer. There are resulting temperature sensitivities of the path (m/K) at each end of a cavity that are proportional to the difference of the coefficient of thermal expansion (α) at the contact. The temperature sensitivity of the resonant frequency can be a minimum at a temperature T_C if the product of length times $\alpha(T_C)$ of the spacer approximately offsets the combined sensitivities of the ends, even if $\alpha(T_C)$ of the spacer is significantly nonzero.

©2009 Optical Society of America

OCIS codes: (020.0020) Atomic and molecular physics; (120.2230) Fabry-Perot; (120.3930) Metrological instrumentation; (160.2750) Glass;

References and links

1. Ch. Eisele, M. Okhapkin, A. Yu. Nevsky, and S. Schiller, "A crossed optical cavities apparatus for a precision test of the isotropy of light propagation," Opt. Commun. **281**(5), 1189–1196 (2008).
2. A. D. Ludlow, X. Huang, M. Notcutt, T. Zanon-Willette, S. M. Foreman, M. M. Boyd, S. Blatt, and J. Ye, "Compact, thermal-noise-limited optical cavity for diode laser stabilization at 1x10$^{(-15)}$," Opt. Lett. **32**(6), 641–643 (2007).
3. ULE and TSG are trademarks of Corning Inc., and mention here is for technical clarity only and does not imply endorsement.
4. S. A. Webster, M. Oxborrow, S. Pugla, J. Millo, and P. Gill, "Thermal-noise-limited optical cavity," Phys. Rev. A **77**(3), 033847 (2008).
5. N. M. Sampas, E. K. Gustafson, and R. L. Byer, "Long-term stability of two diode-laser-pumped nonplanar ring lasers independently stabilized to two Fabry-Perot interferometers," Opt. Lett. **18**(12), 947–949 (1993).
6. N. Poli, R. E. Drullinger, G. Ferrari, M. Prevedelli, F. Sorrentino, M. G. Tarallo, and G. M. Tino, "Prospect for a compact strontium optical lattice clock," Proc. SPIE 6673 (2007).
7. J. Alnis, A. Matveev, N. Kolachevsky, T. Wilken, Th. Udem, and T. W. Hänsch, "Subhertz linewidth diode lasers by stabilization to vibrationally and thermally compensated ultralow-expansion glass Fabry-Pérot cavities," Phys. Rev. A **77**(5), 053809 (2008).
8. S. F. Jacobs, J. W. Berthold, and J. Osmundsen, "Ultraprecise measurement of thermal expansion coefficients – recent progress," AIP conf. Proceedings, New York (1970).
9. M. Notcutt, C. T. Taylor, A. G. Mann, and D. G. Blair, "Temperature compensation for cryogenic cavity stabilized lasers," J. Phys. D Appl. Phys. **28**(9), 1807–1810 (1995).
10. K. Numata, A. Kemery, and J. Camp, "Thermal-noise limit in the frequency stabilization of lasers with rigid cavities," Phys. Rev. Lett. **93**(25), 250602 (2004).
11. J. W. Berthold III, and S. F. Jacobs, "Ultraprecise thermal expansion measurements of seven low expansion materials," Appl. Opt. **15**(10), 2344–2347 (1976).
12. S. F. Jacobs, "Dimensional stability of materials useful in optical engineering," Opt. Acta (Lond.) **33**(11), 1377–1388 (1986).
13. H. Takashashi, "Temperature stability of thin-film narrow-bandpass filters produced by ion-assisted deposition," Appl. Opt. **34**(4), 667–675 (1995).
14. Based on the slope of the phase of the Ta2O5-SiO2 coatings used here, 10 mr/nm, and a spectral shift of such coatings on low expansion glass of $\Delta\nu/\nu \sim\!\!-10^{-5}\ K^{-1}$ [13].
15. A. E. Siegman, Lasers, (University Research Books, 1986).
16. M. Fukuhara, and A. Sampei, "Effects on high-temperature-elastic properties on α-/β-quartz phase transition of fused quartz," J. Mater. Sci. Lett. **18**(10), 751–753 (1999).
17. R. R. VanBrocklin, M. J. Edwards, and B. Wells, "Review of Corning's capabilities for ULE mirror blank manufacturing for an extremely large telescope," Proc. SPIE 6273–01, 1–11 (2006).
18. Fused Silica CTE from 5 – 35 C adapted from the expression in SRM 739: *http://ts.nist.gov/MeasurementServices/ReferenceMaterials/archived_certificates/739.pdf*

#112088 - $15.00 USD Received 1 Jun 2009; revised 22 Jul 2009; accepted 23 Jul 2009; published 10 Aug 2009
(C) 2009 OSA

19. ULE and TSG Product Information Sheets, Corning Advanced Optics, 334 County Rt., 16, Canton, New York 13617 (2006). *http://www.corning.com/docs/specialtymaterials/pisheets/TSGBro91106.pdf http://www.corning.com/docs/specialtymaterials/pisheets/UleBro91106.pdf*
20. M. Edwards, Corning Inc., private communication, $\alpha(T) = K_0 + 2.21T - 0.0122T^2 + 1.88e\text{-}5T^3$ ppb/K, *T* in Celsius (2006).
21. R. W. Fox, "Fabry-Perot temperature dependence and surface-mounted optical cavities," Proc. SPIE 7099 (2008). (available as arXiv:0807.0656v1 [physics.optics]).
22. Ansys Workbench Simulation, V11.0. Mentioned only for technical clarity, no endorsement implied.
23. D. Coyne, "Beamsplitter coating strain induced radius of curvature," LIGO document LIGO-T050057–00-D (2005).
24. M. Okaji, N. Yamada, K. Nara, and H. Kato, "Laser interferometric dilatometer at low temperatures: application to fused silica SRM 739," Cryogenics **35**(12), 887–891 (1995).

1. Introduction

Optical cavities made from low-expansion glasses and optically-contacted high-finesse mirrors are often used as references to stabilize the frequency of lasers in physics experiments and optical clocks [1,2]. For these applications the reference cavity is installed in a vacuum chamber, and usually inside temperature-controlled shielding to minimize frequency fluctuations. ULE, a TiO_2-doped fused silica glass with a temperature dependent coefficient of thermal expansion (CTE) is often used as the cavity spacer material, in particular when operation at or near a temperature that dν/dT equals zero is desired [3]. However, discrepancies between the temperature that dν/dT equals zero, or T_C, and the supposed CTE null of the ULE cavity spacer have been noted numerous times [4–7]. Often, cavities are specified to achieve T_C at a conveniently warm temperature for heating-only control, and the failure to realize the intended T_C means that non-trivial tasks of acousto-optic drift reduction or bi-directional temperature control must be employed to enhance performance [2,7]. Some of these reported discrepancies may be related to structural distortions at the ends of the cavities, for distortion and shifts of T_C due to CTE mismatches between cavity spacers and the mirror substrates have been observed [8,9]. Although mirror deformation [8] and the effect of fused silica mirrors on a sapphire spacer [9] have been treated for particular cavity geometries, no general approach for designing the temperature response of a cavity that includes structural distortion due to optically contacted mirrors has been presented.

This paper presents an approach that should considerably improve predictions of T_C for optical cavities when the material parameters are well known. In fact, there are two requirements for making such predictions: (1) a model of frequency versus temperature that includes all relevant dependences and (2) accurately calibrated CTE values for the glass components. This work focuses mainly on the first issue but has implications for the second. The approach is presented by comparing frequency versus temperature measurements of cavities built with the same spacer but different optically-contacted mirrors to highlight the significance of structural distortion at the ends. Finite element analysis (FEA) is used to make an a priori calculation of this effect. Using the frequency measurements from one cavity, this calculation is used to determine the CTE of the spacer. The results are consistent with the frequency measurements of a second cavity, as well as with those made on a third cavity that was built on this spacer without optical contacting in order to minimize structural distortion. This analysis method should be especially useful in the design of shorter cavities, as end effects have a proportionally larger influence as the cavity length decreases. Furthermore, it may lead to a proper choice of spacer glass to achieve a conveniently warm T_C when fused silica mirror substrates are employed, which is of interest for thermal noise reasons [10]. Such an analysis may also be useful in measurements of the CTE of ultra-low expansion materials, which are sometimes accomplished by monitoring the frequency of optical cavities [11,12].

2. Optical frequency versus temperature

The nominal resonant optical frequencies of the longitudinal modes of a Fabry-perot cavity in vacuum are commonly written

#112088 - $15.00 USD Received 1 Jun 2009; revised 22 Jul 2009; accepted 23 Jul 2009; published 10 Aug 2009
(C) 2009 OSA

$$\nu = \frac{mc}{2l}, \tag{1}$$

with m a unit-less integer denoting the longitudinal mode number. For $\Delta l << l_o$, the dependence of the frequency on length is given by

$$\nu = \nu_o(1-\frac{\Delta l}{l_o}). \tag{2}$$

In this equation l_o is the physical length of the cavity, defined as the distance between the first surfaces of the opposing dielectric stacks, when the frequency of the m^{th} mode is ν_o. An incremental change of the physical length from l_o could occur from expansion of the spacer, which in the case of a constant CTE is given by $\Delta l = l_o\alpha_S\Delta T$. In the more pertinent case of a variable CTE material, Δl is found by integrating $l_o\alpha_S(T)$ over the interval from T_o to T. However, Δl may be due to more than just the spacer's thermal expansion or contraction. Although $l_o\alpha_S(T)$ describes the temperature sensitivity of the spacer in units of m/K, a significant portion of the total temperature sensitivity of l may be due to distortion at the ends, completely independent of the length of the spacer. The familiar expressions of Eqs. (1) and (2) are modified here by including other factors that can affect a mode's resonant frequency, including terms to describe the temperature sensitivity of the cavity length at each end. Taking into account the phase shift upon reflection (φ) due to the mirrors that occurs twice per round-trip, one may write

$$\nu = \frac{c}{2l}(m+\frac{2\phi}{2\pi}). \tag{3}$$

An expression analogous to Eq. (2) is found by taking the derivative of Eq. (3) and explicitly recognizing that Δl has components independent of the spacer's length. Terms accounting for the end sensitivities are written here as $l'_1(T)$ and $l'_2(T)$, also with units of m/K and are temperature dependent since the relative CTE of the mirror, the coatings, and the end of the spacer may be temperature dependent. Thus the modified expression analogous to Eq. (2) includes an integral of the temperature sensitivities of the spacer and both ends in addition to the phase upon reflection term:

$$\nu(T) = \nu_o(1-\frac{1}{l_o}\int_{T_o}^{T} l_S\alpha_S(T)+l'_1(T)+l'_2(T)\ dT)+\frac{c}{2l_o}\frac{\phi'}{\pi}(T-T_o). \tag{4}$$

This is an equation for the cavity frequency as a function of temperature in terms of an initial frequency, ν_o, at an initial temperature T_o. The mirror sagitta are implicitly included here as the difference between l_o and l_S, i.e. $l_o = l_S + 2l_{SAG}$ in the case that both mirrors have the same sagitta. As will be discussed further in the next sections, the temperature sensitivity of a cavity end due to the optically contacted mirror will nearly always be much larger than the unconstrained expansion of the mirror sagitta, or $l'_n(T) >> l_{SAG}\alpha_M$. The phase derivative φ', in units of radians/K, is not temperature dependent over the limited range near room temperature considered here. The second term of Eq. (4) becomes important only for very short cavities since, at least for the hard ion-beam sputtered coatings employed here, the temperature dependence of the phase ($\varphi' \sim -10^{-4}$ rad/K [13,14]) results in a shift of T_C of much less than 1 K for a cavity as short as 10 cm.

The terms $l'_1(T)$ and $l'_2(T)$ account for structural deformation at each end of a Fabry-Perot cavity due to the CTE differences between the mirror substrate and spacer, and to a lesser extent, the coatings. The flat contacting surfaces of the cavity will distort along with the mirror substrate as the constrained components expand differentially. The exact change of the on-axis optical path at each end of a cavity with temperature is likely to be a function of the physical geometry such as the mirror shape, thickness and contacted area, thickness of the coatings, the shape of the spacer near the contact area, and also of the material parameters

#112088 - $15.00 USD Received 1 Jun 2009; revised 22 Jul 2009; accepted 23 Jul 2009; published 10 Aug 2009
(C) 2009 OSA

such as the elastic modulus and Poisson's ratio in addition to the CTE. The temperature sensitivity of each end of the cavity is included individually because the ends may differ, for instance because one end may have a flat mirror that is contacted over a larger area than the opposing curved mirror. Or alternatively, the mirror substrates may be from different lots of glass or even from locations in the same melt that exhibit a different CTE.

This simple model assumes a uniform CTE of each part and a uniform temperature distribution. Small departures from these ideals will be a perturbation on the model results. However it is possible that the transverse spatial variation of the CTE in some spacers may be large enough that bending of the spacer induces a displacement of the mode spot on the mirror, affecting the frequency versus temperature in a manner not accounted for here. Likewise, effects of other variations of the glass such as air inclusions (bubbles) are not taken into account here, nor are dynamic effects that may become important with sufficient optical power circulating in the cavity. Temperature dependence of the Gouy phase [15] and of the glass modulus and Poisson's ratio [16] are not included since these effects are very small. Another influence of temperature on the resonant frequency that is not included in this model may come from the mounting. Strain may develop from the relative movement of fixed mounting points, for instance if a cavity is tightly held at several points by an external structure that has a different CTE than the glass spacer.

The key to this formulism of temperature sensitivities at the cavity ends is a method to approximate $l'_1(T)$ and $l'_2(T)$ with sufficient accuracy. The main problem is that the CTE of both the mirror substrate and the end of the spacer are temperature dependent, and generally different. This will often be the case even if ULE substrates are contacted to a ULE spacer, for the glass specifications allow for as much as a 60 ppb/K (ppb = x 10^{-9}) difference in CTE between two samples. The CTE curve of fused silica and CTE bounds of the low-expansion glasses ULE and TSG [3] are given in Fig. 1. (The average CTE of a given length of glass

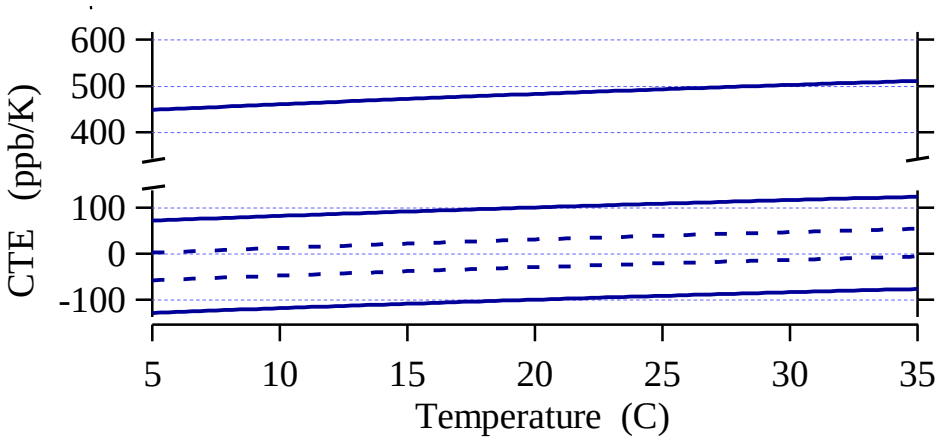

Fig. 1. (Top) Nominal CTE of fused silica per NIST Standard Reference Material 739 [18]. (Lower) CTE bounds of ULE (dashed) and TSG. The ULE(TSG) glass specifications state that within the range of 5 to 35 C, the mean value of the CTE is within the limits of ± 30 (± 100) ppb/K [19]. The nominal temperature dependence, which is given graphically in references [12] and [19], is approximately $\alpha(T) = K_0 + 2.21T - 0.0122T^2$ ppb/K [20] over this limited temperature range shown. No data concerning the statistical variability of the higher-order coefficients of the CTE was found during this work.

exhibits a curve parallel to and within the bounds shown, dependent upon the TiO_2 concentration [17]). A further difficulty is the mechanical strain due to the HR coating. The extremely low-loss ion-beam-sputtered quarter-wave stacks used in high-finesse cavities have a higher modulus than the glass and a much larger CTE.

#112088 - $15.00 USD Received 1 Jun 2009; revised 22 Jul 2009; accepted 23 Jul 2009; published 10 Aug 2009
(C) 2009 OSA

3. Experiment

Optically contacting mirrors of different materials to the same spacer can readily reveal the effect of structural distortion. Here, a single TSG glass spacer was used with pairs of fused silica and ULE mirrors to form two cavities, and resonant frequency versus temperature was monitored using an Iodine-stabilized HeNe laser as a reference. The spacer was 98.04 mm in length, 25.4 mm in diameter with a 6.3 mm diameter borehole and an air relief hole. The ends were polished to $\lambda/10$ flatness for optical contacting. In addition, the outside of the cylinder had a slight flat of width 9 mm that was ground along the spacer length as shown in Fig. 2. No information concerning the CTE of this particular piece was known other than the general TSG glass specifications.

First, fused silica mirrors (Corning 7980 standard grade) were contacted to the ends of the spacer to form a cavity resonant at 633 nm, and frequency versus temperature data was collected as detailed in ref [21] (this reference incorrectly states the spacer length as 99 mm). The high-finesse mirrors were 25.4 mm in diameter, 5.75 mm thick with a 50 cm radius of curvature and the SiO_2/Ta_2O_5 layers were coated by ion-beam sputtering, as was the backside AR coating. An annular flat region for optical contacting extended from a central diameter of 19.1 mm to the chamfered edge, and the resulting sagitta at the center was 91 μm.

Next, the fused silica mirrors were carefully removed from the TSG spacer and a set of ULE mirrors contacted. These substrates had the same geometry and had the same coatings as the fused silica mirrors but were 5.96 mm thick. No information was known about the CTE of the ULE substrates. As with the prior test, the frequency was recorded with the cavity inside a thick-walled blackbody cell while the outside temperature of the vacuum chamber was very slowly changed over the course of approximately 70 hours. The temperature was monitored by the same thermistor still affixed directly to the TSG spacer with a small (< 1 mm^3) quantity of epoxy. Traces of longitudinal mode frequency of the two cavities over a temperature range limited by the experimental set-up are shown in Fig. 2. A potential systematic error exists if the rate of temperature change was insufficiently small, due to the lag between the

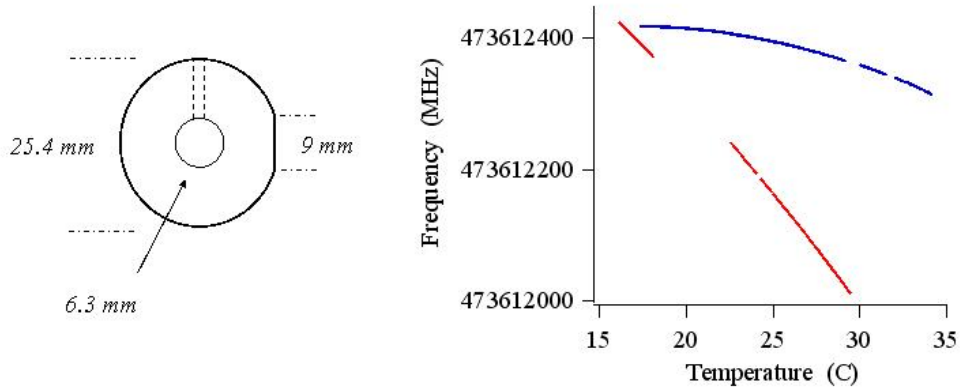

Fig. 2. (Left) A cross section of the 98.04 mm long spacer. (Right) Red: optical frequency versus temperature of a cavity mode with fused silica mirrors contacted. Blue: frequency of a cavity mode with ULE mirrors contacted to the same spacer. The missing data are times when the laser is unlocked.

temperature indication on the surface of the spacer and the actual temperature distribution inside the glass components. This would likely affect the fused silica data more than the ULE data since the dimensional change per degree is much larger.

Clearly the frequency data is not consistent with a simple picture of expansion of the spacer and mirror sagitta without distortion of the geometry. In each cavity the mirror sagitta (91 μm) account for less than 0.2% of the total cavity length. Yet the frequency traces

#112088 - $15.00 USD Received 1 Jun 2009; revised 22 Jul 2009; accepted 23 Jul 2009; published 10 Aug 2009
(C) 2009 OSA

corresponding to the ULE and fused silica mirrors form parabolic curves that peak at $T_C = +16.6$ and $T_C \cong -15 \pm 5$ C respectively. Instead, as will be concluded in the following section, the outward displacement at the center of the constrained fused silica mirror per degree is much larger (≅ 3 nm/K) than would be expected of a simple expansion of the mirror radius sagitta (≅ 40 pm/K).

4. Finite Element Analysis

Our FEA package was not designed to handle calculations over a temperature interval if the CTE values are temperature dependent [22]. (Although the CTE may be entered into the software as a function of temperature, over a temperature interval from T_1 to T_2 only the value $\alpha(T_2)$ is used). However, if the appropriate constant CTE values are assumed for each component, the on-axis temperature sensitivity of the end of a cavity at a discrete temperature can be readily calculated. Each FEA analysis modeled a spacer with one HR coated mirror attached with no slippage of the optical contact. The spacer was held by specifying the opposing flat surface of the spacer as a fixed support, and the general procedure was as follows here. First, CTE values were assigned to the spacer, mirror substrate and HR coating, α_S, α_M and α_C respectively. Next, the displacement of the center of the coating surface along the optical axis due to a + 1 K temperature shift was calculated. Finally, a second FEA calculation with the substrate and coating suppressed determined the change in the length of the spacer itself in the absence of end distortion. Although the change in the FEA spacer's length in one degree may be closely approximated by $l_S\alpha_S$, the second calculation was performed instead as there is a small perturbation of the length caused by constraining the end with a fixed support. The difference between the two FEA calculations yields l'_n, the change of the cavity length per K due to the structural changes at one end corresponding to these static values of α_S, α_M, and α_C. An example calculation output is shown in Fig. 3.

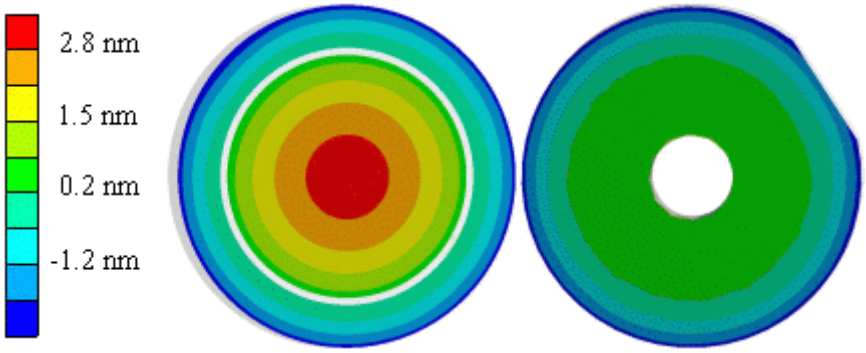

Fig. 3. The FEA graphical results of deformation in the direction of the optical axis caused by a + 1 K temperature change for the case of a 5.75 mm thick fused silica mirror contacted to the one inch diameter spacer, with $\alpha_S = 0$ ppb/K and $\alpha_M = 520$ ppb/K. The range of the color bar is + 3.5 nm to –2.5 nm, with positive numbers indicating an elongation of the cavity. (Left) The coated mirror with the spacer hidden. The center of the coating moves + 3.2 nm/K in the z direction, while the contacted area (outside the white ring) distorts in the opposite direction. (Right) The end of the spacer with the coating and substrate hidden.

A caveat to this analysis is that the CTE differences must be such that a linear relationship exists between stress and strain, i.e., Hooke's Law must apply. The stress at the optical contact region was investigated using FEA under the condition that the CTE difference between the spacer and a substrate was 620 ppb/K, the most expected from a fused silica mirror on a low-expansion substrate. With a temperature shift of 15 K the maximum stress was found to be less than 1% of the tensile strength. Consequently, the stress/strain relationship should be linear in the range of 20 ± 15 C for the mirror configurations analyzed in this work.

#112088 - $15.00 USD Received 1 Jun 2009; revised 22 Jul 2009; accepted 23 Jul 2009; published 10 Aug 2009
(C) 2009 OSA

An elastic modulus and Poisson's ratio of 67.6 GPa and 0.17 respectively are used for the ULE and TSG glass in these calculations, and 72.7 GPa and 0.16 respectively for fused silica. The coating was modeled as a single 5 μm thick layer. Following work on the effective parameters of ion-beam sputtered Ta_2O_5/SiO_2 thin-film coatings, the HR coating parameters ascribed here are a modulus of 106 GPa, a Poisson's ratio of 0.21, and a temperature-independent CTE equal to 1.8×10^{-6} K^{-1} [23]. Care was taken to ensure appropriate finite-element mesh sizes consistent with the sizes of the three parts and the area of the two interfaces. A mesh of 50,000 finite elements was employed, and increasing the number of elements changed the typical result by 0.1%.

With the CTE of each glass part specified by a temperature dependent polynomial, the on-axis distortion at the end of a cavity structure as a function of temperature may be found in the manner described above by assigning the appropriate CTE values and repeating the calculation procedure at a sufficient number of distinct temperatures. However, if a different spacer or mirror glass CTE is considered during the cavity design process, a new set of FEA calculations is necessary. Alternatively, the observation that the on-axis distortion (and subsequent change in T_C [9]) is proportional to the CTE difference between a mirror substrate and the spacer offers a way to avoid additional FEA calculations. The on-axis distortion is linear with respect to $\alpha_M - \alpha_S$ for a given physical structure and material parameters but does but not depend on the absolute value of either CTE. Figure 4 shows the distortion calculated for arbitrary values of α_M and α_S that are expected within the temperature range of interest. To extract numbers from the graphical output a cursor was placed manually at the center of the coating. The possible error from a slight misplacement of the probe from the center was small relative to the l'_n magnitudes, but likely contributed to the residuals shown in Fig. 4.

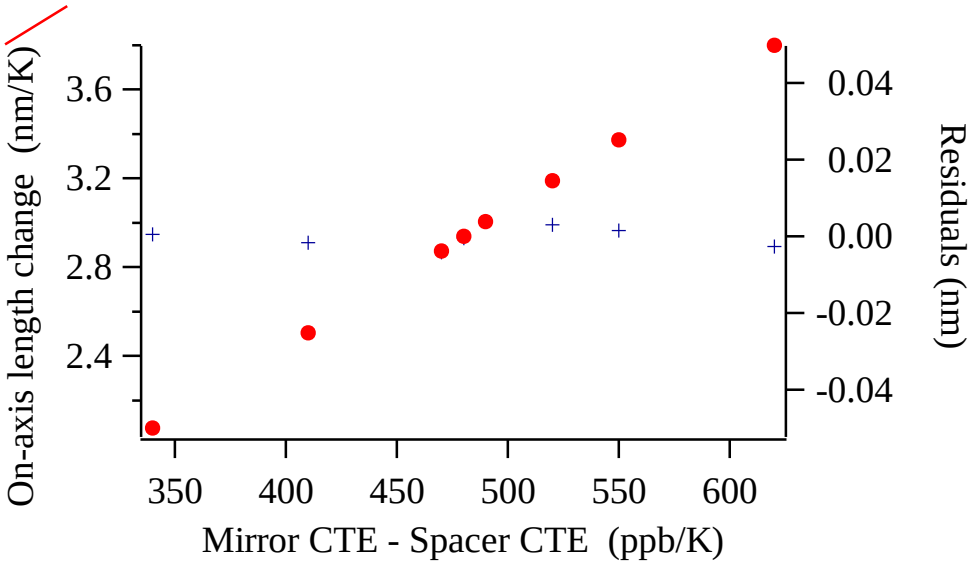

Fig. 4. The temperature sensitivity of one end of a cavity as a function of the CTE difference between a fused silica mirror and the TSG spacer shown in Fig. 2. Red dots, calculated l'_n values for the case of a 25.4 mm diameter, 5.75 mm thick mirror with the geometry and coating described in the text. A linear fit, and the fit residuals (crosses, right axis) are also shown.

The linear dependence of the end distortion on the CTE difference can be established from two or more points by determining the coefficients to Eq. (5).

$$l'_n(T) = A(\alpha_M - \alpha_S) + B. \qquad (5)$$

The coefficients are thus independent of the CTE of the spacer and the substrates, but unique to the physical geometry, the elastic modulus and Poisson's ratio and the coating parameters.

#112088 - $15.00 USD Received 1 Jun 2009; revised 22 Jul 2009; accepted 23 Jul 2009; published 10 Aug 2009
(C) 2009 OSA

The temperature dependence of l'_n follows naturally since the CTE of each part may be expressed as, for instance, $\alpha = K_0 + K_1T + K_2T^2$.

With coated fused silica mirrors and spacer of the dimensions given, the calculations shown in Fig. 4 are described by $l'_n(T) = [0.00616(\alpha_M - \alpha_S) - 0.03] \times 10^{-9}$ m/K, with the CTE in ppb/K. The identical calculation was performed for the case of the slightly thicker ULE mirror, and in that case the result is $l'_n(T) = [0.00596(\alpha_M - \alpha_S) - 0.04] \times 10^{-9}$ m/K.

Initial calculations included a fourth part, a thin (250 nm) AR coating on the substrate's back side. By simulations of the frequency versus temperature, using Eq. (4), it was observed that introducing the AR coating to the model of these 6 mm thick mirrors caused T_C of the 10 cm long cavity to shift by much less than 100 mK. Consequently the AR coating is neglected here.

5. Comparison with experiment

The hypothesis presented is that the cavity mode's frequency versus temperature behavior can be predicted by Eq. (4) in conjunction with FEA calculations of the end's temperature sensitivity. This hypothesis can be tested by comparing Eq. (4) to parabolic frequency measurements of a single cavity, but only if the absolute CTE of the spacer glass is known with certainty. Evaluating Eq. (4) against measurements gleaned from different mirrors on the same spacer that are conducted over a wide temperature range would allow independent conclusions of the spacer CTE to be compared, thus testing the hypothesis. That is the route followed here, except that the data traces shown in Fig. 2 are over a limited temperature span. Comparing any two polynomials (such as Eq. (4) and a measured frequency profile) over a limited range of the independent variable is difficult since a good fit can be obtained for a range of any one coefficient as long as the other coefficients are allowed sufficient freedom. This problem is avoided here by accepting the well established CTE curvature of the spacer glass (Fig. 1), and comparing only the absolute value (or y-intercept) of the spacer's CTE that each frequency measurement indicates. In fitting Eq. (4) to each data trace of Fig. 2 only one free parameter was adjusted, the coefficient K_0 of the polynomial defining the spacer's absolute CTE at 0 C.

The CTE of fused silica is taken as $\alpha_M(T) = 435.1 + 2.66T - 0.014T^2$ ppb/K, with T in Celsius, which was derived from the more complicated exponential expression of ref [18] over the temperature range from 5 – 35 C. All of the remaining terms in Eq. (4) have been given previously except for ν_0 and T_0, which were selected at random from the frequency versus temperature data pairs. Of course, uncertainty of the "best fit" K_0 of the spacer CTE results from uncertainty in the CTE of the mirror substrates.

The fused silica measurements and material uncertainty of –30 to + 30 ppb/K [18] correspond to a range of zero crossings of the spacer's CTE curve from 17 to 22 C respectively (Fig. 5, between the red traces). Likewise, the ULE measurements and mirror substrate uncertainty (K_0 of ULE is between –68.5 and –8.5 ppb/K) leads to a range of probable zero crossings of the same spacer from about 14.6 to 19 C respectively (between the blue traces), and partially overlapping the fused silica results in the region from 17 to 19 C.

The fused silica and ULE measurements taken together indicate that the spacer CTE crosses zero between 17 and 19 C. Notably, a second reference of the CTE of fused silica at 273 K [24] is in agreement with reference [18] only if $\alpha_M(0) < 420$ ppb/K, corresponding to the upper portion of the band between the red traces in Fig. 5 that partially overlaps with the ULE results. Finally, frequency versus temperature of a third cavity built on this spacer was measured previously [21]. As described in the reference, the mirrors were not contacted on the ends of the spacer, but instead were lightly bonded to the flat of the spacer shown in Fig. 2 in a manner designed not to provide stability but to minimize differential thermal expansion between the glass parts. The frequency versus temperature peaked at T_C ~17.5 C, in excellent agreement with the overlapping region of Fig. 5.

#112088 - $15.00 USD Received 1 Jun 2009; revised 22 Jul 2009; accepted 23 Jul 2009; published 10 Aug 2009
(C) 2009 OSA

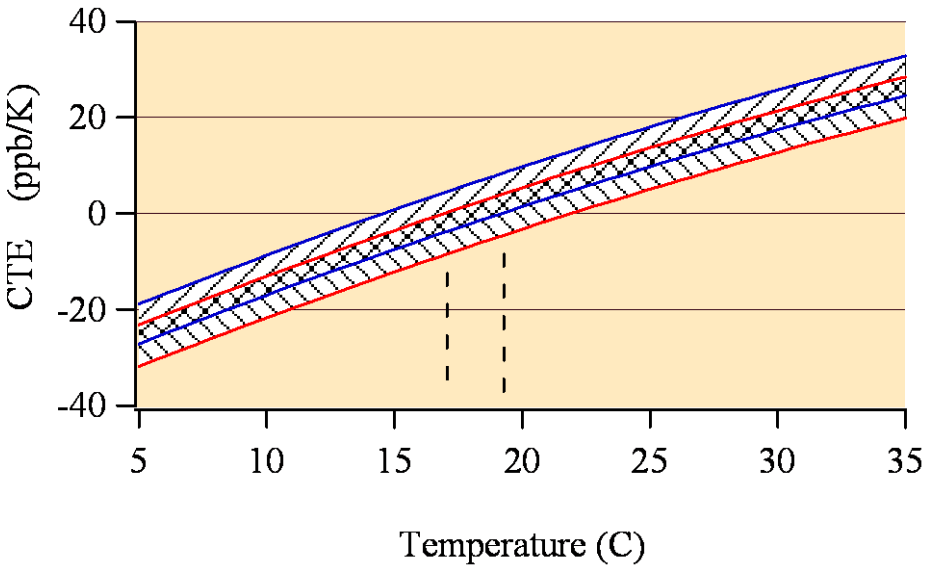

Fig. 5. The spacer CTE as deduced from a fit to the frequency data of Fig. 2 using Eq. (4) and the FEA calculations of end distortion. The expansivity, or curvature of the spacer's CTE is assumed as given in Fig. 1 and only the absolute value (y-intercept) is solved for. The band between the red traces is the range of the spacer CTE resulting from a fit to the cavity data with fused silica mirrors contacted. Similarly, the band between the blue traces is the range of the spacer CTE resulting from a fit to the cavity data with ULE mirrors contacted. In both cases the width of the uncertainty band is due to the mirror CTE uncertainty. Consistent with both measurements are CTE curves that cross zero CTE between 17 and 19 C (cross hatched).

6. Summary

This study demonstrates an important step towards being able to accurately predict T_C, the temperature that dv/dT equals zero, during the design of an optical cavity. Finite element analysis was used to calculate the effects of thermal structural deformation, which is often neglected but can be significant. Equation (4) shows that T_C of the cavity occurs approximately at the temperature at which the sum $l_S\alpha(T) + l'_1(T) + l'_2(T)$ equals zero, which is not likely to be exactly at the CTE null of the spacer. This approach should be useful for tailoring T_C of existing cavities by enabling the proper design of new mirrors. In particular it may also allow the specification of an appropriately negative CTE spacer glass to allow a warm T_C when fused silica mirrors are contacted. Limited additional analysis has shown that, other parameters being equal, the end distortion $l'_n(T)$ becomes smaller as either the mirror thickness is increased or the bore diameter and/or mirror annulus inner diameter are reduced. Also, $l'_n(T)$ trends larger as the diameter of a cylindrical spacer is increased, at least until about two to three times the mirror diameter. This is because for a fixed mirror size a smaller diameter spacer distorts more radially, relieving some of the stress that would otherwise bend the mirror if it was contacted to a larger, stiffer cylinder. Thus the tapered end on some cavity designs [2] serves to reduce $l'_n(T)$ somewhat compared to cylinders. Further experiments with mirrors of different sizes or shapes would be useful in exploring the accuracy to which these methods can be employed to predict frequency versus temperature. The author acknowledges many helpful comments and/or access to resources from Andrew Ludlow, Leo Hollberg, Chris Oates, and Jim Bergquist of NIST, and Prof. Stephen Jacobs at the University of Arizona. This work was supported in part by NIST length metrology funding and this paper is a contribution of an agency of the US government and is not subject to copyright.

#112088 - $15.00 USD Received 1 Jun 2009; revised 22 Jul 2009; accepted 23 Jul 2009; published 10 Aug 2009
(C) 2009 OSA